

# Presumed Inhibitory Neurons in the Macaque Inferior Temporal Cortex: Visual Response Properties and Functional Interactions With Adjacent Neurons

Hiroshi Tamura,<sup>1,2</sup> Hidekazu Kaneko,<sup>2</sup> Keisuke Kawasaki,<sup>1,3</sup> and Ichiro Fujita<sup>1,3</sup>

<sup>1</sup>Graduate School of Frontier Biosciences, Osaka University, Toyonaka, Osaka, 560–8531; <sup>2</sup>National Institute of Advanced Industrial Science and Technology, Tsukuba, Ibaraki, 305–8566; and <sup>3</sup>Core Research for Evolutional Science and Technology, Japan Science and Technology Corporation, Toyonaka, Osaka, 560–8531, Japan

Submitted 29 December 2003; accepted in final form 2 January 2004

**Tamura, Hiroshi, Hidekazu Kaneko, Keisuke Kawasaki, and Ichiro Fujita.** Presumed inhibitory neurons in the macaque inferior temporal cortex: visual response properties and functional interactions with adjacent neurons. *J Neurophysiol* 91: 2782–2796, 2004. First published January 7, 2004; 10.1152/jn.01267.2003. Neurons in area TE of the monkey inferior temporal cortex respond selectively to images of particular objects or their characteristic visual features. The mechanism of generation of the stimulus selectivity, however, is largely unknown. This study addresses the role of inhibitory TE neurons in this process by examining their visual response properties and interactions with adjacent target neurons. We applied cross-correlation analysis to spike trains simultaneously recorded from pairs of adjacent neurons in anesthetized macaques. Neurons whose activity preceded a decrease in activity from their partner were presumed to be inhibitory neurons. Excitatory neurons were also identified as the source neuron of excitatory linkage as evidenced by a sharp peak displaced from the 0-ms bin in cross-correlograms. Most inhibitory neurons responded to a variety of visual stimuli in our stimulus set, which consisted of several dozen geometrical figures and photographs of objects, with a clear stimulus preference. On average, 10% of the stimuli increased firing rates of the inhibitory neurons. Both excitatory and inhibitory neurons exhibited a similar degree of stimulus selectivity. Although inhibitory neurons occasionally shared the most preferred stimuli with their target neurons, overall stimulus preferences were less similar between adjacent neurons with inhibitory linkages than adjacent neurons with common inputs and/or excitatory linkages. These results suggest that inhibitory neurons in area TE are activated selectively and exert stimulus-specific inhibition on adjacent neurons, contributing to shaping of stimulus selectivity of TE neurons.

## INTRODUCTION

Visual information regarding the shape and surface characteristics of objects is processed along the cortical pathway projecting to the inferior temporal cortex in the primate brain. Neurons in area TE of the inferior temporal cortex exhibit selectivity to shapes, and some respond preferentially to complex object images such as faces (Desimone et al. 1984; Gross et al. 1972; Perrett et al. 1982; Tanaka et al. 1991). TE neurons are also selective for color, texture, and binocular disparity (Fujita 2002; Janssen et al. 2000; Komatsu et al. 1992; Sáry et al. 1995; Uka et al. 2000; Wang et al. 2003). A proportion of neurons require that these visual attributes are combined with

specific shapes to achieve maximal activation. The prestriate areas V2 and V4 and area TEO of the inferior temporal cortex also contain a substantial population of neurons that respond more strongly to higher-order shapes, such as crosses and hyperbolic or polar gratings than to bars, edges, or linear gratings (Gallant et al. 1993; Hegdé and Van Essen 2000; Kobatake and Tanaka 1994; Pasupathy and Connor 1999). The stimuli necessary for maximal activation of neurons in these areas, however, are generally less complex than those that excite TE neurons.

The mechanism of generation of stimulus selectivity displayed by TE neurons remains largely unknown. We have recently shown that inhibitory neuronal interactions mediated by the type-A receptor for  $\gamma$ -aminobutyric acid (GABA) shape multiple characteristics of the visual response (Wang et al. 2000, 2002, 2003). Removal of this inhibition by local application of a GABA<sub>A</sub> receptor antagonist, bicuculline methiodide, to TE neurons modulates their stimulus-selective responses. Bicuculline application augments responses to a subset of stimuli, even unmasking responses to stimuli that do not elicit responses under normal conditions. Responses to other stimuli, including some of the originally effective stimuli, remain unaffected.

Several types of local inhibitory circuitry can explain stimulus-specific effect of bicuculline. A straightforward interpretation is that inhibitory neurons are stimulus selective. However, stimulus-specific inhibition may not entail inhibitory neurons with stimulus-specific responses; such inhibition can occur if inhibitory neurons with poor stimulus tuning shunt stimulus-specific excitatory inputs. Broadband inhibition can be mediated by stimulus-selective inhibitory neurons selective for different stimuli that converge onto a same target neuron. To separate these possibilities, we need to investigate the response properties of individual inhibitory neurons. Such a study directly addresses if the responses of inhibitory neurons are stimulus selective and how this stimulus selectivity is related to that of their target neurons.

In the present study, we identified inhibitory neurons by applying cross-correlation analysis to extracellular spikes recorded simultaneously from adjacent neurons. A paired neuron the activity of which was followed by a decrease in activity of its partner was presumed to be inhibitory. Most of the inhibi-

Address for reprint requests and other correspondence: H. Tamura, Laboratory for Cognitive Neuroscience, Graduate School of Frontier Biosciences, Osaka University, Toyonaka, Osaka, 560–8531, Japan (E-mail: tamura@fbs.osaka-u.ac.jp).

The costs of publication of this article were defrayed in part by the payment of page charges. The article must therefore be hereby marked “advertisement” in accordance with 18 U.S.C. Section 1734 solely to indicate this fact.

tory neurons had clear stimulus preferences. Overall the stimulus preferences of inhibitory neurons differed from that of their target neurons. The results suggest that inhibitory TE neurons are involved in shaping stimulus preferences by providing stimulus-specific inhibition. Part of the present results has appeared in abstract form (Tamura et al. 2002).

## METHODS

Neuronal responses were recorded from area TE of the inferior temporal cortex in four anesthetized monkeys (*Macaca fuscata*; body weight, 5.2–7.5 kg). All the experimental procedures were in accordance with the guidelines of the National Institutes of Health (1996) and the Japan Neuroscience Society. The Osaka University Animal Experiment Committee, with a veterinarian as a committee member, approved the procedures as appropriate and conforming to the current standard of the animal experiment protocols.

### Preparation

General experimental procedures were similar to those described previously (Wang et al. 2002). Monkeys were prepared for recordings through an initial aseptic surgery, which began with an injection of atropine sulfate (0.1 mg/kg im) and ketamine hydrochloride (12 mg/kg im). For 12 h before introducing anesthesia, monkeys were deprived of food. Water was freely available. Electrocardiogram (ECG) and arterial oxygen saturation levels were continuously monitored throughout the surgery. The heart rate is continuously audiomonitored. Body temperature was maintained at 37–38°C. A vasotropic drug (Adona, Tanabe; 1.0 mg/kg im) and an anti-plasmin agent (Transamine, Dai-ichi; 17 mg/kg im) were given to minimize bleeding during the surgery. We inserted an intravenous tube into a vein and infused 5% glucose-saline at a speed of 25 ml/h. The infusion fluid contained 131 Na<sup>+</sup>, 4 K<sup>+</sup>, 3 Ca<sup>2+</sup>, 110 Cl<sup>-</sup>, and 28 lactate<sup>-</sup> (mEq/l). Anesthesia was induced and maintained by pentobarbital sodium (15 mg/kg iv) through the intravenous tube. Spontaneous change in the heart rate, cardiac responses, and body movements were carefully monitored. Anesthesia was supplemented by additional injections of pentobarbital sodium (5 mg/kg iv each) when necessary. After topical application of local anesthetic (2% lidocaine), a head restraint was attached with acrylic resin onto the top of the skull. In each monkey, only the right side of the lateral surface of the skull was exposed and covered with resin. The right zygomatic arc was partially (<5 mm) removed to access the anterior part of area TE. An antibiotic (Pentacilin, Sankyo; 40 mg/kg im) and an antiinflammatory/analgesic agent (Voltaren, Novartis; or Ketoprofen, Chugai Pharmaceutical) were given after the surgery and also during the first postoperative week.

After 1–2 wk of recovery, the eye optics were assessed to select appropriate contact lenses allowing images to be focused on the retina at a distance of 57 cm from the cornea. Photographs of the retinal fundus were taken to determine the position of the fovea.

### Recordings

The monkeys were first injected with atropine sulfate (0.1 mg/kg im) and then ketamine hydrochloride (12 mg/kg im). After we applied local anesthetic (1–5 sprays of lidocaine; 8 mg/spray) to pharynx and larynx, an endotracheal cannula, lubricated with a coating of local anesthetic (2% lidocaine) and anti-infective/antiinflammatory (Chlomy-P ointment, Sankyo), was inserted into trachea. The animals were held through the head restraint. No painful procedures such as using a stereotaxic apparatus were applied for the purpose of holding them. The animals were then anesthetized by inhalation of 2–3% isoflurane in 70% N<sub>2</sub>O-30% O<sub>2</sub> through the endotracheal cannula (Popilskis and Kohn 1999). ECG and arterial oxygen saturation levels were continuously monitored throughout the experiment. The heart

rate was continuously audiomonitored. Body temperature was maintained at 37–38°C. We infused 5% glucose-saline at a speed of 25 ml/h through an intravenous tube. Atropine sulfate (0.005 mg · kg<sup>-1</sup> · h<sup>-1</sup>, intravenous) was administered to reduce salivation. We drilled a small hole in the skull (~5 mm), made a small slit (0.5–1 mm) in the dura, and penetrated an electrode (100 μm in the shaft diameter; see Fig. 1A) into the brain through the slit.

After the completion of surgical procedures, we carefully decreased the concentration of isoflurane to 0.5–1% in 70% N<sub>2</sub>O-30% O<sub>2</sub>, the minimal level at which the animals did not respond to external stimuli such as a sudden touch to the facial skin. We also consulted previous literatures about the dose of isoflurane for visual physiology experiments (Pack et al. 2001; Sato et al. 1996; Tigwell and Sauter 1992; Tsunoda et al. 2001). To immobilize eye movements for visual physiology experiments, the animals were paralyzed with pancuronium bromide (0.02 mg · kg<sup>-1</sup> · h<sup>-1</sup>, intravenous) diluted in the 5% glucose-saline. The monkeys were artificially ventilated through the endotracheal cannula at the rate of 25 strokes/min. The volume of a single stroke of ventilation was adjusted to keep end-tidal CO<sub>2</sub> level being at 4.0–4.5% and was usually ~80 ml. During the experiments, we continuously paid attention to spontaneous changes in the heart rate and cardiac responses to touches to the skin with a cotton tip by an experimenter. We increased the concentration of isoflurane if the heart rate increased >10% on touching the skin (Sato et al. 1996). Under this anesthetic condition, the heart rate was maintained at 142 ± 20 (SD) beats/min. Arterial oxygen saturation level was always >95% and was 99% on average. These physiological parameters, i.e., heart rate, body-temperature, end-tidal CO<sub>2</sub>, and arterial oxygen saturation level were comparable to the ones reported in functional brain-imaging studies using anesthetized monkeys (Logothetis et al. 1999). We did not observe any signs of arrhythmia or edema, which may be induced by an imbalance of electrolyte or blood volume. We also watched urination.

The anesthetic protocol described in the preceding text decreased the firing rates of neurons in area TE; the maximum firing rate of our neurons recorded from anesthetized animals [11.5 ± 12.3 (SD) spikes/s] was substantially lower than that of neurons recorded from alert animals (35.0 ± 27.9 spikes/s, mean) (awake animals of Tamura and Tanaka 2001). However, other properties such as stimulus selectivity have been shown to be largely preserved in anesthetized animals (Rodman et al. 1991; Kato et al. 1999; Tamura and Tanaka 2001).

The pupils were dilated and the lenses were relaxed by the local application of 0.5% tropicamide-0.5% phenylephrine. Corneas were covered with preselected contact lenses, which had artificial pupils of 3 mm diam. They prevented eyes from drying. Further, we irrigated eyes every 20–60 min with saline.

Multiple single-unit recordings were made from area TE using a single-shaft electrode with seven recording probes (Fig. 1A; Heptode; Thomas, Germany). Due to the technical details of our custom-made software, we used six of the seven probes, including the tip probe, for recording. The impedance of each probe was 1–2 MΩ at 1 kHz. The electrode was advanced with a manipulator (Narishige, Tokyo) from the side to the cortical surface. Recorded potentials were amplified 10,000 times, band-pass filtered (500 Hz to 3 kHz), and digitized at a 50-μs resolution, then stored on a computer for later analysis. Using the electrode, the action potentials (“spikes”) generated by a single neuron were recorded by some or all of the six recording probes simultaneously with different amplitudes and waveforms. Each individual probe could record spikes from multiple neurons. The isolation and classification of single neuronal activity are described in the following text. Recordings were made at intervals of ≥300 μm along a penetration axis so as not to sample the same neurons at successive sites. The sampling diameter of each probe was estimated at 150 μm (Kaneko et al. 1998). All neurons encountered were recorded and analyzed. At the end of a recording session in each penetration, two or three small electrolytic lesions were made by passing a cathodal

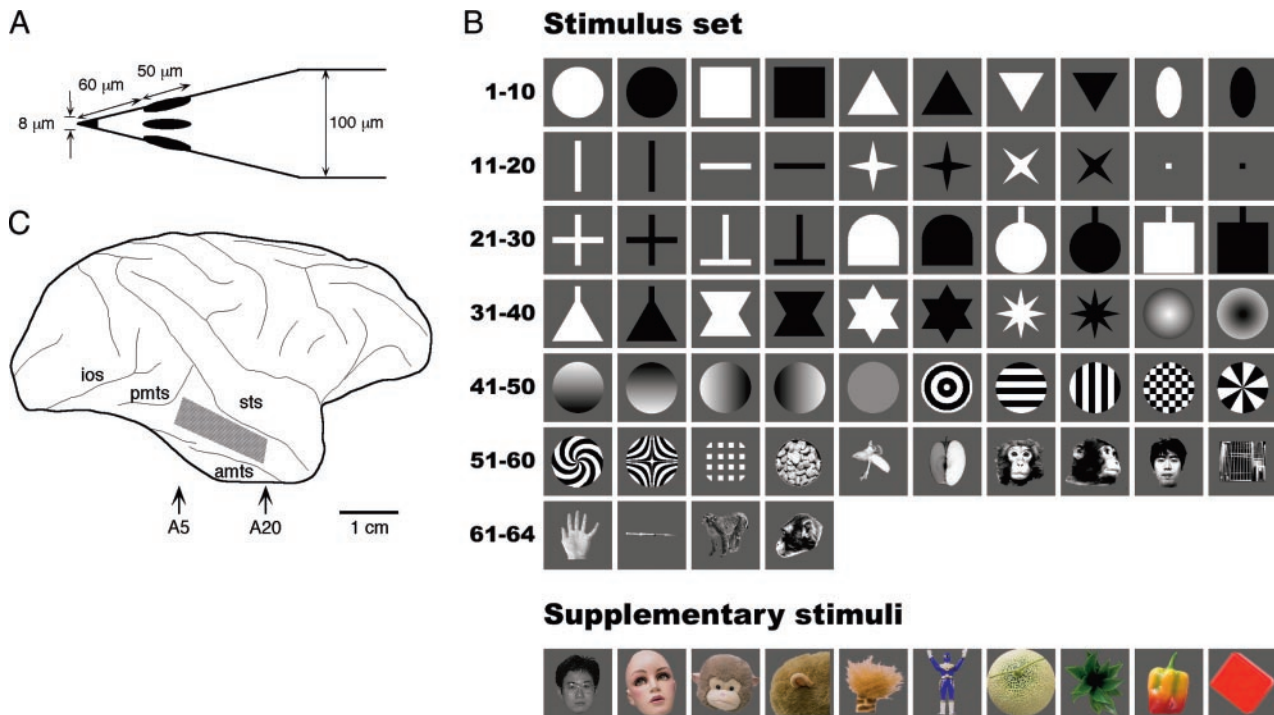


FIG. 1. Electrode, stimulus images, and recording site. *A*: the electrode (Heptode; Thomas, Germany) has 7 recording probes. One probe is at the tip; the other 6 surround the electrode at a distance of  $60\ \mu\text{m}$  from the tip. *B*: the top 64 images constitute the predetermined stimulus set routinely used for every neuron, whereas the lower 10 images are examples of supplementary stimuli used for neurons unresponsive to the routine set. *C*: the shaded area on the lateral view of the right cerebral hemisphere indicates the overall recording site in all animals. The area corresponds to the dorsal part of area TE. amts, anterior middle temporal sulcus; ios, inferior occipital sulcus; pmts, posterior middle temporal sulcus; sts, superior temporal sulcus. A5 and A20 indicate levels 5 and 20 mm anterior to the ear canal.

current of  $10\ \mu\text{A}$  through the electrode tip for 10 s to allow later histological verification of the recording sites.

Each recording session lasted for 10–15 h after which the hole in the skull was cleaned and filled with resin. We washed eyes with saline and administered a drop of antibiotics (Tarivid ophthalmic solution, Santen, 3 mg/ml) and a drop of vitamin B<sub>2</sub> (Flavitan eye drops, Yamanouchi, 0.5 mg/ml). Within 20–30 min after the termination of muscle relaxant infusion, spontaneous respiration resumed and returned to normal, aided by an injection of neostigmine methylsulfate (Vagostigmine, Shionogi; 0.1 mg/kg im). Monkeys were returned to their home cages after antibiotic injection (Pentacilin, Sankyo; 40 mg/kg im).

### Visual stimuli

The stimulus set used routinely consisted of 64 visual stimuli (Fig. 1*B*, stimulus set), 53 two-dimensional geometrical shapes (circles, squares, triangles, bars, stars, gradation patterns, gratings, etc.) and 11 photographs of natural or man-made objects (banana, apple, monkey face, human face, cage, hand, syringe, etc.). Images were  $\leq 4^\circ$  in visual angle and were encoded in 256 gray levels. The luminances of white and black were 99.2 and 0.7  $\text{cd}/\text{m}^2$ , respectively. If none of the 64 stimuli activated multiple-unit activities recorded from the tip probe during the initial survey, we searched for effective visual stimuli by presenting a collection of objects, including laboratory items and plastic or stuffed toys of animals and plants. We then added these effective images to the routine set (Fig. 1*B*, supplementary stimuli). These stimuli were encoded in 24-bit color depth. On average, 68 stimuli (64 routine and 4 supplementary stimuli) were presented to the animals for each recording site. The maximum response magnitude and “signal” correlation (see following text for definition) did not differ among neurons presented with a different number of stimuli ( $P > 0.05$ , Mann-Whitney’s  $U$  test).

Visual stimuli were presented individually for 1 s against a homogeneous gray background ( $15.7\ \text{cd}/\text{m}^2$ ) at the center of the receptive field hand-plotted for each recording site by referring to audiomonitored multiple-unit activities recorded from the tip probe. The same homogeneous gray field was presented during the 1-s intervals between presentations of stimuli. The stimuli were presented in a pseudorandom order within a stimulus presentation block. Ten blocks were presented for each recording site.

### Isolation and classification of spikes

Isolation and classification of spikes from recorded signals were carried out by an automatic method described previously (Kaneko et al. 1999). Spikes in the recorded signal were detected by matching with a template spike. The covariance value between the template spike and a detected spike was then calculated for each of the six recording probes. The six-covariance values were vectorized and analyzed by hierarchical clustering using a multidimensional statistical test (Lance and Williams 1967). A cluster of covariance values in six-dimensional space corresponds to spikes from a single neuron; different neurons yielded different clusters. The following procedures were taken to minimize possible errors in single-unit isolation (Kaneko et al. 1999). Errors due to partially overlapping spikes were minimized by successively subtracting the preceding spikes from raw signal to recover the shape of subsequent spikes. Clustering errors due to bursts of progressively smaller spikes were avoided by detecting such bursts, then using only the first spike in each burst for clustering. After assigning the first spike to a particular neuron, the remaining spikes in the burst were assigned to the same neuron.

For the purposes of this study, the multiprobe recording technique has several advantages over conventional single-probe recording techniques. First, it allows us to reliably isolate and analyze low-amplitude spikes from inhibitory neurons, which generally have small dendritic

arbors. Second, the technique also enables recording from a single neuron for long durations, thereby increasing the number of recorded spikes and allowing sensitive detection of inhibitory connections between pairs of neurons by cross-correlation analysis (see following text; Aertsen and Gerstein 1985). These two advantages increase the likelihood that inhibitory neurons are reliably recorded.

### Analysis of visual responses

The statistical significance of a response was determined by comparing the firing rate obtained during a 1-s period starting 80 ms after the onset of stimulus presentation with the spontaneous firing rate during a 0.4-s period immediately before stimulus onset ( $P < 0.05$ , Wilcoxon's signed-rank test). The magnitude of a response to a given stimulus was computed as the mean firing rate during visual stimulation minus the mean spontaneous firing rate over 10 trials. For a given pair of neurons, overall similarity in stimulus preference was assessed by signal correlation, which was quantified as Pearson's correlation coefficient ( $r$ ) between two sets of the response magnitudes (signal) to a stimulus set (Gawne and Richmond 1993). We evaluated the stimulus selectivity of individual neurons as the proportion of stimuli that evoked responses  $>25\%$  of the maximal neuronal response. We also counted the number of effective stimuli that evoked statistically significant responses ( $P < 0.05$ , Wilcoxon's signed-rank test) in individual neurons.

### Cross-correlation analysis

Functional connectivity between a pair of simultaneously recorded neurons was assessed by cross-correlation analysis (Perkel et al. 1967). Cross-correlograms (CCGs) were computed by accumulating spike occurrence times in one neuron relative to the spikes of the paired neuron. Spikes were continuously collected during visual stimulation and the interstimulus period, a total collection period of  $\geq 1,280$  s ( $2 \text{ s} \times 64 \text{ stimuli} \times 10 \text{ blocks}$ ). 3,736 spikes (median; range, 570–58,249) were collected during this period. Original spike trains were convolved by a Gaussian function ( $\sigma = 0.4$  ms) to decrease high-frequency components and re-sampled at 0.4-ms bins. A CCG was then constructed with temporal resolution of 0.4 ms for the period spanning from  $-0.2$  to  $0.2$  s.

As visual stimulation activated two neurons almost simultaneously, a raw CCG reflected both correlation due to the stimulus-locked activation (stimulus coordination) and correlation due to functional connections between the two neurons (neural correlation). To separate these contributions, we calculated a shift-predicted CCG, which is obtained by shifting the time relation of spike trains between the two neurons by one trial (Perkel et al. 1967; Toyama et al. 1981). A shift-predicted CCG was calculated for individual stimulus conditions; these values were pooled for each pair of neurons. The feature, either a peak or a trough, that was produced by stimulus coordination appears both in a raw CCG and a shift-predicted CCG. A feature derived from neural interaction only appears in a raw CCG. Hence, we can distinguish the two features and isolate the neural correlation component.

Spike counts in each bin from a raw CCG and a shift-predicted CCG were compared statistically ( $P < 0.0001$ , binomial test) within a time window of  $\pm 12.6$  ms (63 bins) to detect a feature within a raw CCG. As our spike classification method cannot separate spikes that occur  $<0.2$  ms apart, spike counts at 0-ms bin of the raw CCGs are 0 in principle, causing an artificial trough to appear. The convolution of spike trains with the Gaussian function ( $\sigma = 0.4$  ms), however, provides the spike counts at 0-ms bin; thus the artificial trough is less visible in some CCGs. As the convolution broadens the artificial trough, negative deviations within  $\pm 1.0$  ms ( $2.5 \sigma$ ; 5 bins) were ignored during analysis. Thus the statistical test of features in CCG was performed for each of the 58

bins, and the probability that a feature exceeds the statistical criteria ( $P < 0.0001$ ) by chance is 0.0058.

Peaks and troughs appearing in a raw CCG but not in a shift-predicted CCG were interpreted as indications for different types of neuronal interactions (Bryant et al. 1972; Hata et al. 1990; Menz and Freeman 2003; Moore et al. 1970; Perkel et al. 1967; Toyama et al. 1981; Ts'o et al. 1986). Serial inhibitory linkage yields a trough displaced from the 0-ms bin. Significant troughs ( $P < 0.0001$ ) appearing within  $-12.6$  to  $-1.0$  ms or  $1.0$  to  $12.6$  ms were interpreted as inhibitory functional interactions based on the previous studies that examined cortical inhibitory synaptic interactions (Komatsu et al. 1988; Matsumura et al. 1996). Two troughs with one appearing on each side of the 0-ms bin were not considered as an indication of mutual inhibitory interaction because other possibilities can explain the feature. Common inputs and/or excitatory linkages can yield peaks in the CCGs. We interpreted only the significant peaks ( $P < 0.0001$ ) that do not straddle the 0-ms bin, that reach their peak within 3.4 ms and that have a peak width at half height  $<10$  ms as indicating the presence of serial excitatory linkage (Menz and Freeman 2003; Toyama et al., 1981). We interpreted other significant peaks ( $P < 0.0001$ ) that occurred within  $\pm 12.6$  ms as products of common inputs to both neurons. Two sharp peaks with one appearing on each side of the 0-ms bin were not interpreted as products of mutual excitation but as products of common inputs because these peaks were likely to be produced by a combination of a center peak and an artificial trough at the 0-ms bin that derived from our spike classification method.

We defined the nadir of CCG trough and the peak of CCG peak as the largest differences in spike counts between the raw CCG and the shift-predicted CCG within the time window of  $\pm 12.6$  ms and their timing as the latencies. We measured the trough width as a consecutive time period around its nadir during which spike counts in each bin of raw CCG were numerically lower than corresponding counts of shift-predicted CCG. Similarly, the peak width was defined as a consecutive time period around the peak during which spike counts in each bin of raw CCG were higher than corresponding counts of shift-predicted CCG. Trough or peak area was defined as the integrated difference in spike counts between raw and shift-predicted CCGs during the consecutive time period. Strength of the functional interaction was represented by the area normalized by the geometric mean of total spike counts of neurons in a pair (Constantinidis et al. 2001; Gochin et al. 1991; Toyama et al. 1981).

### Histology

After completion of the final recordings, monkeys were killed with pentobarbital sodium and perfused from the heart with 4% paraformaldehyde. The brain was then removed and cut into 100- $\mu\text{m}$ -thick serial sections for reconstruction of electrode penetrations. Penetrations and recording sites were reconstructed using the combination of the electrolytic lesions and the electrode manipulator readings noted for each recording site.

We successfully recovered all the electrolytic lesions from Nissl-stained sections. Neuronal activities were recorded in an area spanning from 5 to 20 mm anterior to the external ear canal in the dorsal part of the inferior temporal cortex (*monkey 1*: 6–18 mm; *monkey 2*: 8–18 mm; *monkey 3*: 5–20 mm; *monkey 4*: 13–15 mm; Fig. 1C). Because the most posterior penetrations in each monkey contained neurons with a large receptive field spanning  $>20^\circ$  of visual angle and including the fovea (Kawasaki et al. 2000), we considered that our penetrations were within area TE (Boussaoud et al. 1991; Tanaka et al. 1991). The mediolateral extent ranged from the ventral lip of the superior temporal sulcus (sts) to the lateral lip of the anterior middle temporal sulcus (amts). The area examined corresponded to the dorsal part of area TE (Tamura and Tanaka 2001).

## RESULTS

We analyzed 1,028 neuron pairs obtained from 455 neurons at 103 sites in area TE of four monkeys. Two to 12 neurons (median = 4) were isolated at a single recording site. If three or more neurons were isolated from a single recording site, neurons were analyzed as multiple neuron pairs.

*Functional properties of presumed inhibitory neurons*

The neuron of a pair that induced a displaced trough in CCG is presumed to be inhibitory. Two examples of neuron pairs (Fig. 2, A–D and E–H) demonstrate a trough displaced in one direction from the 0-ms bin in the raw CCG. The patterns of spike amplitudes across six probes of a Heptode were different

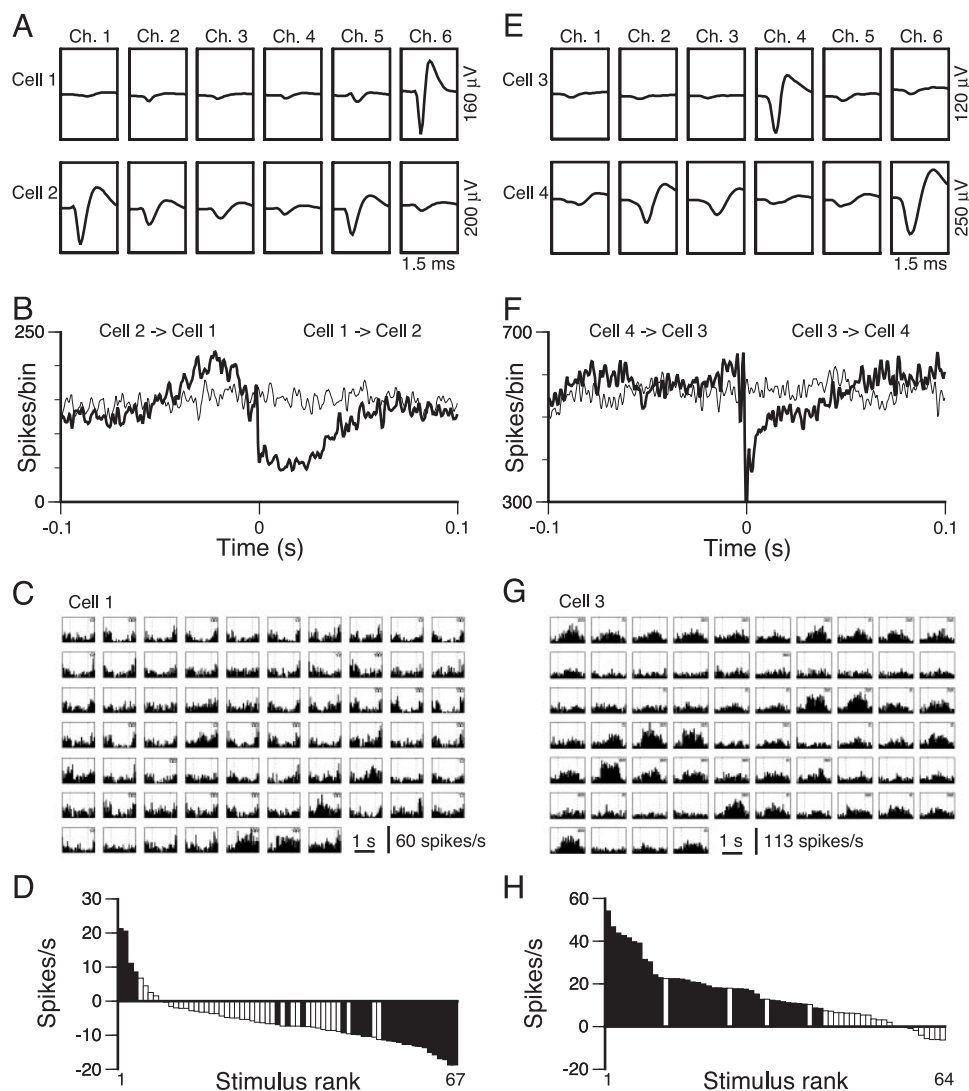


FIG. 2. Two examples (A–D, E–H) of identification of inhibitory neurons in area TE by cross-correlation analysis. A: the average spike shapes of *cells 1* and *2* recorded from 6 probes of a Heptode are shown separately. *Cell 1* was recorded from channel 6 of a Heptode with the maximal amplitude. *Cell 2* was recorded from channel 1 of the Heptode with the maximal amplitude. B: cross-correlogram (CCG) exhibiting a trough displaced from the 0-ms bin. The CCGs, covering  $\pm 0.1$  s with 0.4-ms bins, represent the number of spikes that occurred in *cell 2* before (left side of the CCG) and after (right side of the CCG) spikes generated in *cell 1* (reference). The raw (thick line) and shift-predicted (thin line) CCGs are shown. Spike counts in a several bins at and around 0 ms of raw CCG are underestimated because of the technical limitation (see METHODS for details). Number of spikes: 19,520 for *cell 1* and 7,224 for *cell 2*. C: peri-stimulus time histograms (PSTHs) of *cell 1*, an inhibitory neuron, to a set of visual stimuli, including the routine set stimuli (Fig. 1B) and an additional image of a human face in grayscale (stimulus 65), in color (stimulus 66), and in black-and-white (stimulus 67). The initial 64 responses are arranged in the same order as the predetermined 64 stimuli in Fig. 1B. The responses of the neuron to the 3 remaining responses to images of human faces were appended. Vertical dotted lines indicate onset and offset of visual stimulus presentation. Stars within a graph indicate significance levels (single star,  $0.01 \leq P < 0.05$ ; double star,  $P < 0.01$ , Wilcoxon's signed-rank test). D: response profile of the inhibitory neuron (*cell 1*) to the 67 stimuli. The responses are arranged in stimulus rank order. Closed and open columns indicate statistically significant ( $P < 0.05$ , Wilcoxon's signed-rank test) and nonsignificant responses, respectively. E: average spike shapes of another neuron pair (*cells 3* and *4*). *Cell 3* was recorded from channel 4 of a Heptode with the maximal amplitude. *Cell 4* was recorded from channel 6 with the maximal amplitude. F: CCG with a trough displaced from the 0-ms bin. The CCGs cover  $\pm 0.1$  s with 0.4-ms bins. Spike counts in several bins at and around 0 ms of raw CCG are underestimated because of the technical limitation (see METHODS for details). Number of spikes: 33,409 for *cell 3* and 17,342 for *cell 4*. G: PSTHs of *cell 3*, an inhibitory neuron, to the predetermined set of stimuli. H: response profile of the inhibitory neuron (*cell 3*) to the 64 stimuli.

between the two neurons in a pair, thus discriminating each of the neurons (Fig. 2, *A* and *E*). In the neuronal pair displayed in Fig. 2, *A–D*, the trough in the raw CCG (thick line) displaced toward the positive direction from the 0-ms bin (Fig. 2*B*). This trough was not observed in the shift-predicted CCG (thin line), indicating an inhibitory influence of the reference cell (*cell 1*) on the other cell (*cell 2*). The trough persisted for 60 ms. The peak appearing on the left side of the raw CCG may be caused by either a primary synaptic effect, such as an excitatory linkage from *cell 2* to *cell 1* and/or common inputs to both neurons or a secondary effect. Possible secondary effects could include presynaptic dead time (Bryant et al. 1972) in which, just before the firing of an inhibitory neuron, the inhibitory neuron cannot fire due to the refractory period, leading to increased excitability of the target neuron. From this CCG, therefore we identified *cell 1* as an inhibitory neuron, but the nature of *cell 2* was unclear.

The spike amplitude, measured from the base line to the initial negative nadir, was 91.4  $\mu\text{V}$  (Fig. 2*A*, *cell 1*). The spike width, measured from the initial negative nadir to the subsequent positive peak, was 252  $\mu\text{s}$  for the inhibitory neuron (Fig. 2*A*, *cell 1*). The spontaneous firing rate of the inhibitory neuron was 16.7 spikes/s during the 0.4-s period immediately prior to stimulus onset. The maximum response amplitude, defined as the largest change in firing rate from the spontaneous activity, was 21.3 spikes/s. Four of the 67 stimuli tested increased the firing rate of the inhibitory neuron, whereas 23 stimuli decreased it ( $P < 0.05$ , Wilcoxon's signed-rank test; Fig. 2, *C* and *D*). The proportion of stimuli that evoked responses  $>25\%$  of the maximal response of the inhibitory neuron was 0.07 (5 of 67 stimuli, Fig. 2*D*). *Cell 2* had spike amplitude of 72.1  $\mu\text{V}$  and spike width of 482  $\mu\text{s}$  (Fig. 2*A*, *cell 2*). Visual responses of the target neuron (*cell 2*) will be described in the following text.

Another inhibitory neuron (*cell 3*, Fig. 2, *right*) exhibited broader stimulus selectivity than *cell 1*. The trough displaced toward the positive direction from the 0-ms bin (Fig. 2*F*) indicates an inhibitory influence of the reference cell (*cell 3*) on the other cell (*cell 4*); the reference cell was presumed to be an inhibitory neuron. The spike amplitude and spike width of the inhibitory neuron were 52.5  $\mu\text{V}$  and 380  $\mu\text{s}$ , respectively (Fig. 2*E*), and the spontaneous firing rate was 18.9 spikes/s. The maximum response amplitude of the inhibitory neuron was 54.2 spikes/s. Thirty-seven of the 64 stimuli increased the firing rate of this neuron, whereas none of the stimuli decreased it ( $P < 0.05$ , Wilcoxon's signed-rank test; Fig. 2*G*). The proportion of stimuli that evoked responses  $>25\%$  of the maximal response of the neuron was 0.45 (29 of 64 stimuli, Fig. 2*H*). *Cell 4* had spike amplitude of 103.0  $\mu\text{V}$  and spike width of 621  $\mu\text{s}$  (Fig. 2*A*, *cell 2*).

To compare the properties of inhibitory neurons with those of excitatory neurons, we identified excitatory neurons by cross-correlation analysis. Raw CCGs with a sharp peak displaced from the 0-ms bin were interpreted as the product of a direct excitatory linkage between neurons. The source neuron of this kind of linkage is presumed to be excitatory. An example of a neuron pair demonstrates a peak displaced in one direction from the 0-ms bin in the raw CCG (Fig. 3). Neurons were isolated based on the patterns of spike amplitudes across six probes of a Heptode (Fig. 3*A*). The latency of the displaced peak in the CCG was 1.6 ms with a width at half-height of 2.8 ms (Fig. 3*B*), indicating an excitatory influence of the reference

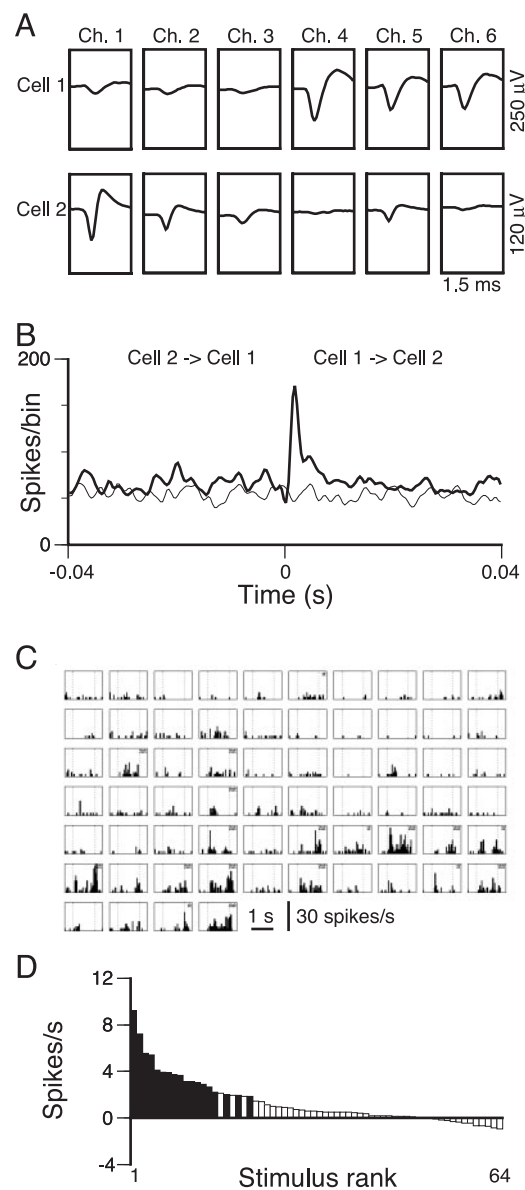


FIG. 3. Identification of an excitatory neuron in area TE by cross-correlation analysis. *A*: average spike shapes of *cells 1* and *2* recorded from a Heptode. *Cell 1* was recorded from channel 4 of a Heptode with the maximal amplitude. *Cell 2* was recorded from channel 1 with the maximal amplitude. *B*: CCG with a sharp peak displaced from the 0-ms bin, covered  $\pm 0.04$  s with 0.4-ms bins. Spike counts in several bins at and around 0 ms of raw CCG are underestimated because of the technical limitation (see METHODS for details). Number of spikes: 1,593 for *cell 1* and 20,318 for *cell 2*. *C*: PSTHs of *cell 1*, an excitatory neuron, to the predetermined set of stimuli. *D*: response profile of the excitatory neuron (*cell 1*) to the 64 stimuli. Other conventions are as in Fig. 2.

cell (*cell 1*) on the other cell (*cell 2*). Spike amplitude and width of the excitatory neuron were 83.3  $\mu\text{V}$  and 612  $\mu\text{s}$  (Fig. 3*A*, *cell 1*). The spontaneous firing rate and the maximum response of the excitatory neuron were 0.5 and 9.2 spikes/s respectively. Eighteen of the 64 stimuli increased the firing rate of the excitatory neuron, whereas no stimuli decreased it ( $P < 0.05$ , Wilcoxon's signed-rank test; Fig. 3, *C* and *D*). The proportion of stimuli that evoked responses  $>25\%$  of the maximal response of the excitatory neuron was 0.22 (14 of 64 stimuli, Fig. 3*D*).

Among the 1,028 neuron pairs examined by cross-correlation analysis, a large number of pairs (397) exhibited a peak straddling the 0-ms bin. These common-input pairs may also involve direct excitatory and/or inhibitory linkages between the neurons, although the presence of common-input peaks obscured the features derived from these direct interactions. We mainly focused our analysis on 56 pairs with a displaced trough, and 20 pairs with a sharp displaced peak without straddling the 0-ms bin in the raw CCGs (see METHODS for the criteria). A low incidence of purely serial excitatory linkages is common in previous cross-correlation studies (Constantinidis et al. 2001; Hata et al. 1990; Toyama et al. 1981; Ts'o et al. 1986; see DISCUSSION). From the present analysis, 49 of the 455 neurons were presumed to be inhibitory, 19 were presumed to be excitatory; the remaining 387 neurons were not classified. The total number of identified neurons (68) was smaller than the number of serial linkage pairs (76) because some neurons were involved in multiple pairings. We never observed a case where a single neuron provided excitation for a target neuron and inhibition for another. The incidences of inhibitory and excitatory neurons were not different along the anterior-posterior axis in the inferior temporal cortex ( $P = 0.120$ ,  $\chi^2$  test).

The incidence of inhibitory neurons responding by increasing their firing rate to at least one of the stimuli (46/49) did not differ from that of excitatory neurons (16/19;  $P = 0.210$ ,  $\chi^2$  test). Likewise the incidence of inhibitory neurons decreasing their firing rate in response to at least one of the stimuli (24/49) did not differ from that of excitatory neurons (9/19;  $P = 0.560$ ,  $\chi^2$  test).

Analysis of population data indicates that inhibitory neurons were as stimulus selective as excitatory neurons (Fig. 4). The stimulus selectivity of individual neurons was evaluated by three measures: the proportion of stimuli that evoked responses >25% of the maximal neuronal response, the proportion of stimuli that increased the firing above the spontaneous firing rate ( $P < 0.05$ , Wilcoxon's signed-rank test), and the proportion of stimuli that decreased firing below the spontaneous firing rate ( $P < 0.05$ , Wilcoxon's signed-rank test). The median of the proportion of stimuli that evoked responses >25% of the maximal response was 0.21 for inhibitory neurons and 0.23 for excitatory neurons. The medians of the proportions of stimuli increasing the firing rates of inhibitory and excitatory neurons were 0.10 and 0.21, respectively. The medians of the

proportion of stimuli that decreased firing rates in inhibitory and excitatory neurons were both 0.04. By these three measures, there were no differences between inhibitory and excitatory neurons ( $P > 0.05$ , Mann-Whitney's  $U$  test) except for the proportion of stimuli increasing the firing rate ( $P = 0.033$ ,  $U$  test). Thus we concluded that the difference in the degree of stimulus selectivity between inhibitory and excitatory neurons was small, if any.

Although many of the properties of these cells were similar, some physiological properties differed between the 49 inhibitory and 19 excitatory neurons (Table 1). No difference was found in the spike amplitude between inhibitory neurons ( $102.4 \pm 46.8 \mu\text{V}$ ) and excitatory neurons ( $98.3 \pm 55.3 \mu\text{V}$ ;  $P = 0.408$ ,  $U$  test). On average, inhibitory neurons exhibited a shorter spike width [ $492.6 \pm 92.1$  (SD)  $\mu\text{s}$ ] than excitatory neurons ( $539.4 \pm 89.4 \mu\text{s}$ ;  $P = 0.040$ ,  $U$  test), although there was a large overlap. The spontaneous firing rate of inhibitory neurons [ $7.4 \pm 7.2$  (SD) spikes/s] was higher than that of excitatory neurons ( $4.5 \pm 5.3$  spikes/s;  $P = 0.027$ ,  $U$  test). Spontaneous firing rates of the identified and the other neurons were plotted against spike widths to see the distributions of identified neurons among the entire sample (Fig. 5) (Constantinidis and Goldman-Rakic 2002). The frequency distribution of spike width of all the 455 neurons was bimodal with a dip located  $\sim 400 \mu\text{s}$ . Sixteen percent of the 455 neurons had spike width  $< 400 \mu\text{s}$  and might correspond to fast-spiking neurons. Of the 49 inhibitory neurons, 8 had spike width  $< 400 \mu\text{s}$ , and they had spontaneous firing rates  $> 4$  spikes/s ( $14.0 \pm 11.3$  spikes/s). Only one of the identified excitatory neurons had a spike width  $< 400 \mu\text{s}$  ( $349.5 \mu\text{s}$ ), but its spontaneous firing rate was low (2 spikes/s; Fig. 5). The maximal visual response of inhibitory neurons ( $12.1 \pm 11.6$  spikes/s), however, did not differ from that of excitatory neurons (Table 1;  $10.6 \pm 7.7$  spikes/s;  $P = 0.897$ ,  $U$  test). Also, the occurrence in inhibitory neurons of the burst discharge, defined as the occurrence of more than one spikes within 1.5- to 10-ms intervals, was not different from that of excitatory neurons ( $P = 0.822$ ,  $U$  test).

The spike width and each of the three measures of stimulus selectivity did not correlate in inhibitory neurons ( $r = -0.17$  to  $0.03$ ,  $P > 0.05$ ). The spike width, however, correlated inversely with the spontaneous firing rate ( $r = -0.35$ ,  $P = 0.014$ ; see Fig. 5) and the maximal response ( $r = -0.47$ ,  $P = 0.001$ ). Inhibitory neurons with shorter spike widths tended to

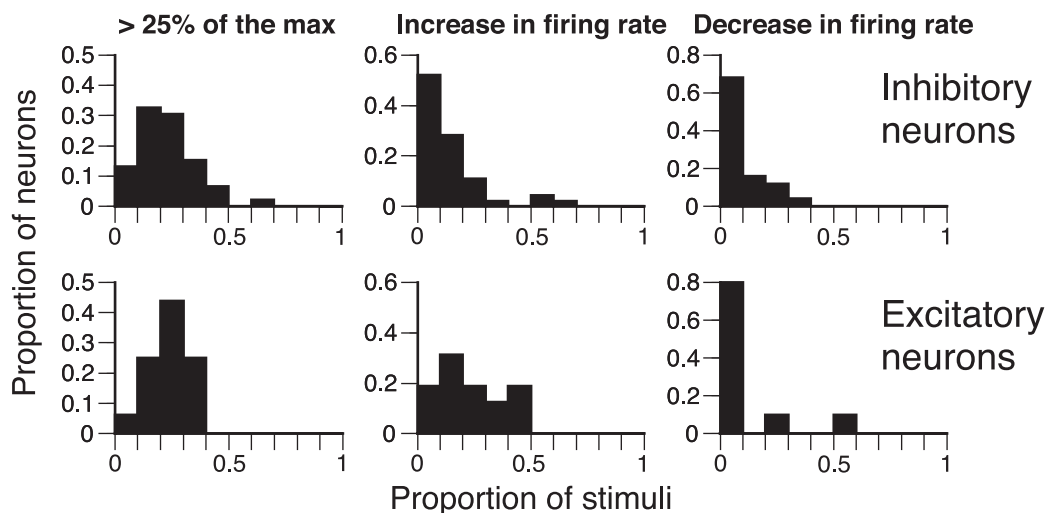


FIG. 4. Comparison of stimulus selectivity between inhibitory and excitatory neurons. The proportion of stimuli that evoked responses >25% of the maximal neuronal response (left), the proportion of stimuli that increased firing rates from spontaneous firing rates in individual neurons (middle), and the proportion of stimuli that decreased firing rates from spontaneous firing rates in individual neurons (right) were compared between inhibitory (top) and excitatory (bottom) neurons. Histograms demonstrated the frequency distributions of these populations of neurons.

TABLE 1. *Physiological properties of presumed inhibitory and excitatory neurons*

	Inhibitory Neurons	Excitatory Neurons
No. of neurons	49	19
Spike amplitude, $\mu\text{V}$	$102.4 \pm 46.8$	$98.3 \pm 55.3$
Spike width, $\mu\text{s}$	$492.6 \pm 92.1$	$539.4 \pm 89.4^*$
Spontaneous firing rate, spikes/s	$7.4 \pm 7.2$	$4.5 \pm 5.3^*$
Maximal response, spikes/s	$12.1 \pm 11.6$	$10.6 \pm 7.7$

Values are mean  $\pm$  SD. For maximal responses, spontaneous firing rate was subtracted. \*:  $P < 0.05$ ,  $U$  test.

exhibit higher spontaneous firing rates and responded to stimuli with a higher firing rate. None of the preceding relationships was observed for excitatory neurons ( $P > 0.05$ ).

The time course of visual responses in inhibitory neurons differed from that in excitatory neurons. The averaged response, calculated across the responses of individual neurons to the respective best stimuli, demonstrated a tonic time course for the inhibitory neurons, whereas a transient component was more prominent in the averaged response of excitatory neurons (Fig. 6;  $P = 0.013$ , discriminant analysis, SPSS Base 9.0, IL 1999).

#### Functional connectivity and response correlation

We next examined similarity in stimulus preference between the presumed inhibitory neurons and their target neurons to see whether inhibitory neurons targeted the other neurons with similar stimulus preferences. One may expect that if a stimulus-selective inhibitory neuron is connected to a neuron, the

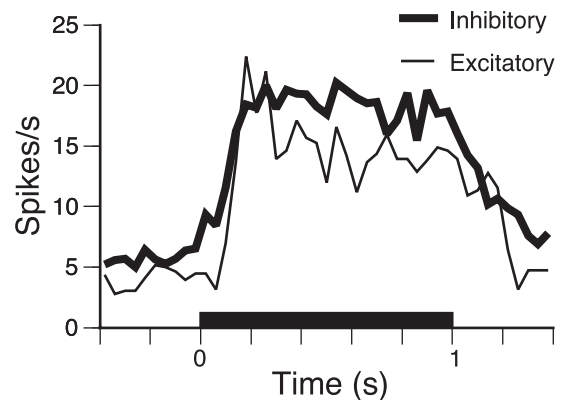


FIG. 6. Averaged time courses of the maximum response of inhibitory (thick line) and excitatory (thin line) neurons. The time courses were obtained by averaging across 49 inhibitory or 19 excitatory neurons. The black bar on the horizontal axis indicates the stimulus presentation period.

target neuron has an inverse stimulus preference. However, this will not necessarily be the case because the contribution of an input from any single neuron to the generation of spikes in a postsynaptic neuron is generally weak in the cortex (Constantinidis et al. 2001; Gochin et al. 1991; Toyama et al. 1981); estimation from CCGs in the present study indicates that a single input spike of an inhibitory neuron, on average, influenced the generation of only 8% of spikes in a postsynaptic neuron.

Some of the neuron pairs with inhibitory linkages exhibited overall stimulus preferences that inversely correlated with each other. An example of such a neuron pair is shown in Fig. 7. This is the neuron pair already discussed in Fig. 2, A–D. A displaced trough in the CCG indicated an inhibitory linkage between them (Fig. 7A). The most preferred stimulus of one neuron was a nonpreferred stimulus of the partner, as shown by their response profiles (Fig. 7B). An image of a human face (open arrowhead) excited *cell 1* maximally but decreased the firing rate of *cell 2*. Conversely, an image of a hand (filled arrowhead) maximally increased the firing rate of *cell 2* but decreased the firing rate of *cell 1*. Pearson's correlation coefficient between the responses of the two neurons to the stimulus set (signal correlation) was  $-0.38$  ( $P = 0.002$ ; Fig. 7C). Another neuron pair with a trough in the CCG also exhibited inversely correlated stimulus preferences ( $r = -0.36$ ,  $P = 0.004$ ; Fig. 8A). An example of pairs with inhibitory linkage demonstrated independent response profiles (Fig. 8B;  $r = 0.12$ ,  $P = 0.328$ ). We also found positively correlated response profiles in pairs with inhibitory linkages (e.g., Fig. 8C;  $r = 0.30$ ,  $P = 0.014$ ).

On the other hand, most of the paired neurons with excitatory linkages or common inputs had similar overall stimulus preferences. Some of them had a high signal correlation that was not observed in pairs with inhibitory linkages. A neuronal pair with an excitatory linkage, shown in Fig. 9A, demonstrated a signal correlation of  $0.30$  ( $P = 0.016$ ). Another neuron pair with a displaced peak also showed a positive signal correlation, although it was not statistically significant ( $r = 0.22$ ,  $P = 0.080$ ; Fig. 9B). A neuron pair with a peak straddling the 0-ms bin, suggesting the presence of common inputs to both neurons, also had a positive signal correlation ( $r = 0.33$ ,  $P = 0.007$ ; Fig. 9C), and another pair with a center peak had highly correlated response profiles ( $r = 0.76$ ,  $P < 0.001$ ; Fig. 9D).

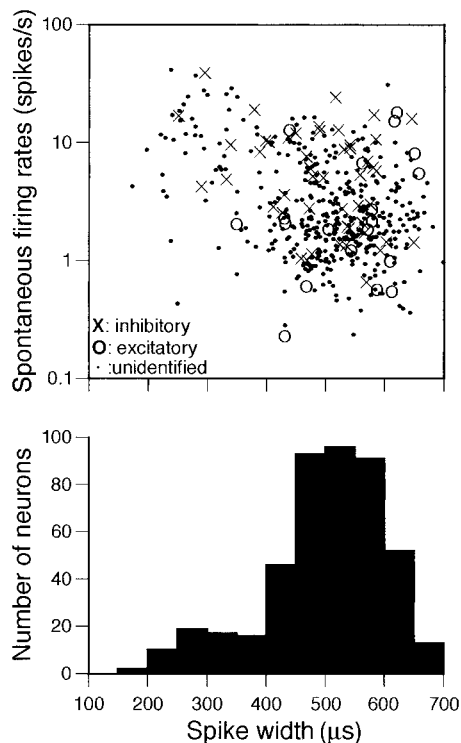


FIG. 5. Scatter plot of spontaneous firing rates against spike width, and frequency distributions of spike width. X, O, and ·: inhibitory, excitatory, and unidentified neurons, respectively.

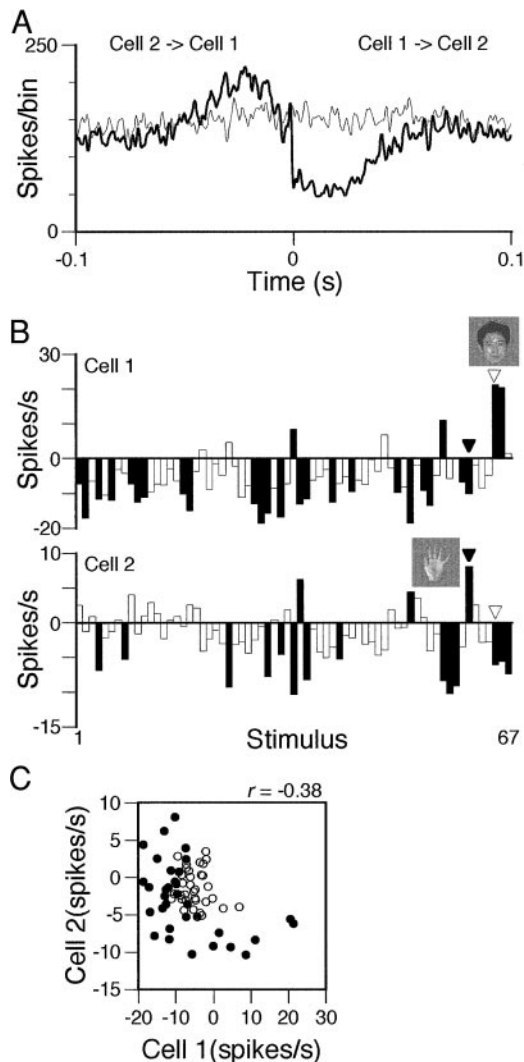


FIG. 7. An example of neuronal pair with an inhibitory linkage. *A*: the CCG from Fig. 2*B* was replicated. *B*: response profiles of *cells 1* and *2* to a set of visual stimuli, including the predetermined 64 stimuli and an additional image of a human face in grayscale (stimulus 65), color (stimulus 66), and black-and-white (stimulus 67).  $\nabla$ , stimulus 65 (inset), which evoked the strongest response in *cell 1*.  $\blacktriangledown$ , stimulus 61 (a photographs of human hand in grayscale, inset), which was the best stimulus for *cell 2*. *C*: signal correlation between the neurons.  $\bullet$ , stimuli, which evoked significant responses in  $\geq 1$  of the neurons.  $\circ$ , ineffective stimuli.

Analysis of all of the samples indicated that neuron pairs with different functional interactions had different degrees of stimulus preference similarities between neurons in a pair. We classified these pairs into three types according to the features of the raw CCGs; neuron pairs with a trough displaced from the 0-ms bin with or without an accompanying peak (inhibitory-linkage pairs,  $n = 56$ ), neuron pairs with a sharp peak displaced from the 0-ms bin without a trough (excitatory-linkage pairs,  $n = 20$ ), and neuron pairs with a peak straddling the 0-ms bin without a trough (common-input pairs,  $n = 397$ ). The average coefficients of signal correlation for pairs with inhibitory linkages, excitatory linkages, and common inputs were  $-0.04 \pm 0.22$ ,  $0.24 \pm 0.25$ , and  $0.18 \pm 0.22$  (means  $\pm$  SD), respectively. The frequency distributions of the signal correlation differed among the three types of neuron pairs ( $P < 0.001$ , Kruskal Wallis test; Fig. 10). Sixteen percent of the pairs with

inhibitory linkages had a significantly ( $P < 0.05$ ) negative signal correlation, and none of the pairs with excitatory linkages and only a small fraction of pairs with common inputs (2%) had significantly negative signal correlation. On the other hand, significant ( $P < 0.05$ ) positive signal correlation was observed in 11, 40, and 37% of inhibitory-linkage pairs, excitatory-linkage pairs, and common-input pairs, respectively. Thus the incidence of negatively correlated or independent overall stimulus preferences was higher for pairs with the inhibitory linkages than those with excitatory linkages or common inputs.

Although the overall distribution of signal correlations differed among pairs with differing CCG types, each type had a variety of degrees in their signal correlation. We then investigated possible relationship between the strength of the functional interaction and the degree of signal correlation in each CCG type. To examine the strength of the functional interaction between neurons, we quantitated the peak or trough area (Constantinidis et al. 2001; Gochin et al. 1991; Toyama et al. 1981). This was measured in a CCG obtained by subtracting the shift-predicted CCG from the raw CCG. The area thus obtained was then divided by the geometric mean of the spike counts of constituent neurons. This analysis showed that the strength of the functional interaction between a pair of neurons was related to the degree of signal correlation. In neuron pairs with inhibitory linkages, the trough area was negatively correlated with the degree of signal correlation ( $r = -0.29$ ,  $P = 0.032$ ). Inhibitory-linkage pairs with inverse stimulus preference exhibited stronger inhibitory interactions than those with similar stimulus preferences. In neuron pairs with excitatory linkages or common inputs, the peak area was positively correlated with the degree of signal correlation ( $r = 0.51$ ,  $P = 0.023$  for excitatory-linkage pairs;  $r = 0.27$ ,  $P < 0.001$  for common-input pairs). Thus excitatory-linkage or common-input pairs with more similar overall stimulus preferences tended to exhibit stronger excitatory interactions or a higher degree of coordinated firing than those with lower similarity of stimulus preferences.

We next examined the congruity of the most preferred stimulus between a pair of neurons. We determined the rank of the most preferred stimulus of a neuron in the partner neuron's stimulus preference. For example, the most preferred stimulus for *cell 1* of Fig. 7 (stimulus 65,  $\nabla$  in Fig. 7*B*) was the 49th ranked stimulus for *cell 2* of Fig. 7, and the most preferred stimulus for *cell 2* (stimulus 61,  $\blacktriangledown$  in Fig. 7*B*) was the 58th ranked stimulus for *cell 1*. Thus we obtained two rank-order values for each pairs. If the most preferred stimulus is shared by two neurons, the rank-order values will be 1 for both neurons. If the most preferred stimulus of a neuron is independent from that of the other as a population, the frequency distribution of rank orders will be uniform. The distribution of 2,056 rank orders from the entire 1,028 pairs was not uniform ( $P < 0.001$ ,  $\chi^2$  test; Fig. 11*A*); 34% (690/2,056) had 1–15th rank orders, indicating that the most preferred stimulus of a neuron often activates adjacent neurons well.

Neuron pairs with different types of CCGs exhibited different patterns of rank-order frequency distributions ( $P = 0.003$ ,  $\chi^2$  test; Fig. 11, *B–D*). The frequency distribution for the inhibitory-linkage pairs exhibited a uniform distribution ( $P = 0.177$ ,  $\chi^2$  test; Fig. 11*B*); inhibitory linkages were observed between neurons regardless of whether or not they shared the

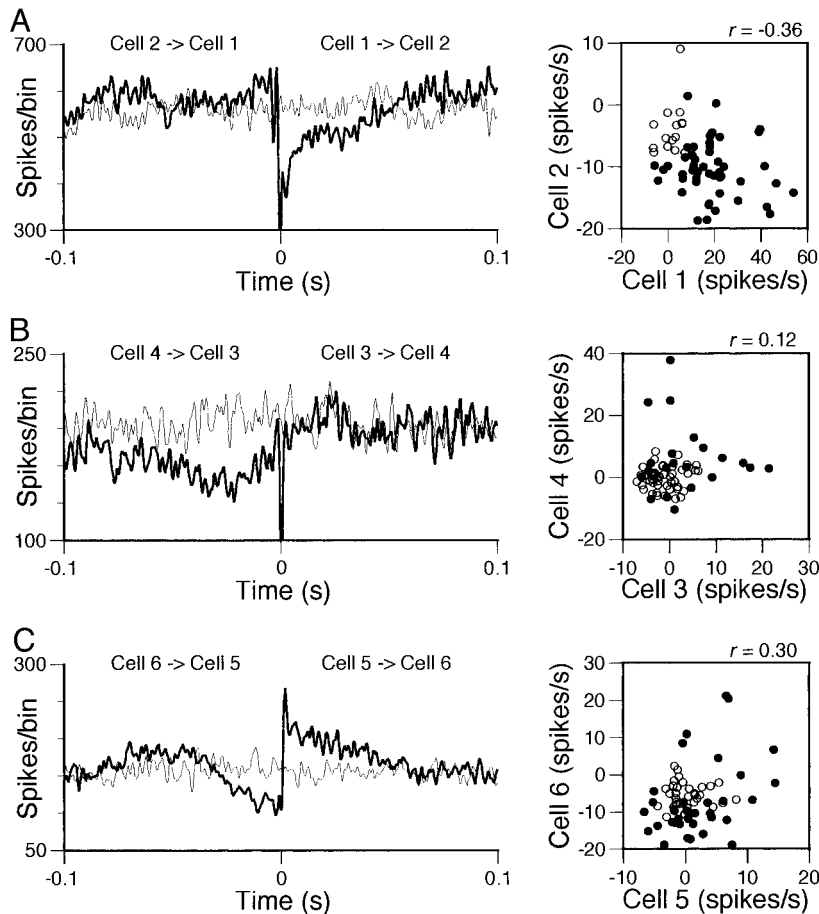


FIG. 8. Three examples of trough-containing CCGs (left) and scatter diagrams of their response magnitudes to the stimulus set (right). CCGs covered  $\pm 0.1$  s with 0.4-ms bins. Signal correlation ( $r$ ) is indicated at the top of the scatter diagrams.  $\bullet$  and  $\circ$ , effective and ineffective stimuli, respectively. A: the CCG from Fig. 2F is replicated. B and C: the trough was displaced in a negative direction, indicating the presence of inhibitory linkage from cell 4 to cell 3 (B) and cell 6 to cell 5 (C). Cell 6 is cell 1 in Fig. 2; a single inhibitory neuron was connected to 2 other neurons. Spike counts in several bins at and  $\sim 0$  ms of raw CCGs are underestimated because of the technical limitation (see METHODS for details). Number of spikes: 12,236 for cell 3, 16,226 for cell 4, 7,901 for cell 5, 19,520 for cell 6.

most preferred stimuli. In contrast, the frequency distribution of the excitatory-linkage pairs was not uniform and skewed toward the 1–15th rank ( $P < 0.001$ ,  $\chi^2$  test; Fig. 11C); the most preferred stimulus of a neuron that constitutes an excitatory-linkage pair was ranked in a higher order, mostly the 1–15th rank group, of a partner neuron. A similar but less conspicuous tendency was observed in common-input pairs ( $P < 0.001$ ,  $\chi^2$  test; Fig. 11D).

We compared the area of troughs or peaks in CCGs among the four different rank-order groups. In the inhibitory-linkage groups, the trough area did not differ among them ( $P = 0.917$ , Kruskal Wallis test). Thus the strength of inhibitory interactions was not reflected in the degree of sharing of the most preferred stimuli but more related to the similarity in overall stimulus preferences (see preceding text). The peak area did not differ among the four rank groups in excitatory-linkage pairs ( $P = 0.543$ ). On the other hand, it differed among the four groups in common-input pairs ( $P < 0.001$ ). Common-input pairs with the shared best stimulus tended to exhibit a higher degree of coordinated firing than those without.

## DISCUSSION

Inhibitory neurons identified on the basis of cross-correlation analysis exhibited stimulus-selective visual responses. The incidence of visually responsive neurons and the degree of stimulus selectivity were comparable between inhibitory and excitatory neurons. Inhibitory neurons tended to connect with neurons with dissimilar overall stimulus preferences, whereas

excitatory neurons exhibited more frequent connections to neurons with shared overall stimulus selectivity.

### Identification of inhibitory and excitatory neurons

A straightforward and decisive method to identify inhibitory neurons *in vitro* is to perform intracellular recording and staining combined with immunohistochemical staining for glutamic acid decarboxylase (McCormick et al. 1985). This method is not readily applicable to *in vivo* experiments, although it is not impossible (Azouz et al. 1997). Previous studies have tried to identify inhibitory neurons from information obtained with extracellular recording techniques. For example, narrow extracellular spikes are associated with fast-spiking inhibitory neurons (e.g., Mountcastle et al. 1969; Simons 1978; Wilson et al. 1994). Constantinidis and Gldman-Rakic (2002) classified cells with higher spontaneous firing rates and narrower spike width as fast-spiking neurons and those with lower spontaneous firing rates and broader spike width as regular-spiking neurons. They assumed those fast-spiking neurons were inhibitory. Our finding that neurons with narrower spike width ( $< 400 \mu\text{s}$ ) and a higher spontaneous firing rate ( $> 4$  spikes/s) were never classified into excitatory neurons on the basis of CCGs was consistent with their classification method. Rao et al. (1999) reported that some regular-spiking neurons were recorded with an electrode over a few hundred micrometers, whereas fast-spiking neurons were rarely tracked for  $> 20 \mu\text{m}$ . Consistent with this, we observed that spikes from excitatory neurons tended to be recorded at many probes with large

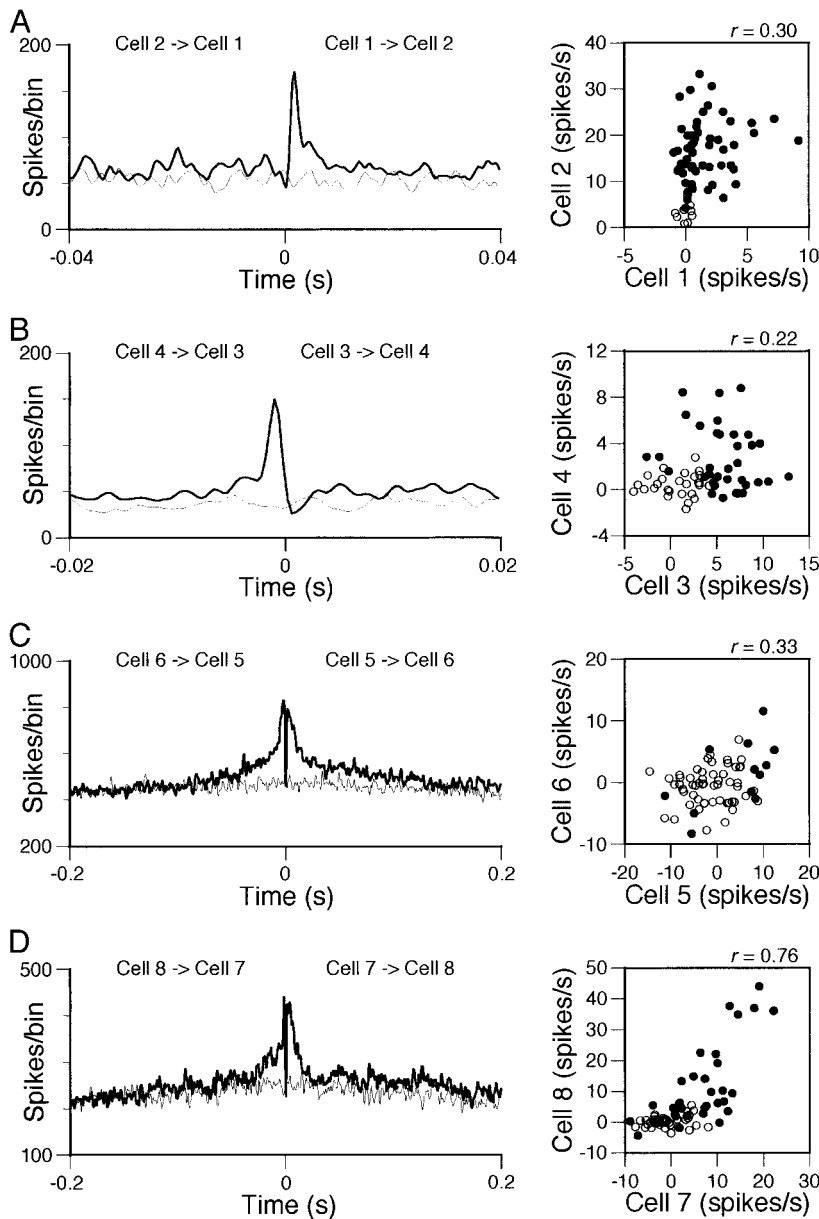


FIG. 9. Four examples of peak-containing CCGs (*left*) and scatter diagrams of their response magnitudes to the stimulus set (*right*). CCGs covered  $\pm 0.04$  s (*A*),  $\pm 0.02$  s (*B*), or  $\pm 0.2$  s (*C* and *D*) with 0.4-ms bins.  $\bullet$  and  $\circ$ , effective and ineffective stimuli, respectively. *A* and *B*: pairs with displaced peak. *A*: the CCG from Fig. 3*B* is replicated. *B*: the peak was displaced in the negative direction, indicating the presence of an excitatory linkage from cell 4 to cell 3. *C* and *D*: pairs with a center peak. Spike counts in several bins at and  $\sim 0$  ms of raw CCGs are underestimated because of the technical limitation (see METHODS for details). Number of spikes: 9,871 for cell 3, 2,529 for cell 4, 34,249 for cell 5, 13,013 for cell 6, 24,909 for cell 7, and 7,638 for cell 8.

amplitudes, whereas spikes from inhibitory neurons tended to be recorded only at a single probe (see Figs. 2 and 3). Cortical inhibitory neurons, however, are highly diverse in their physiology, morphology, and chemistry; other classes of inhibitory

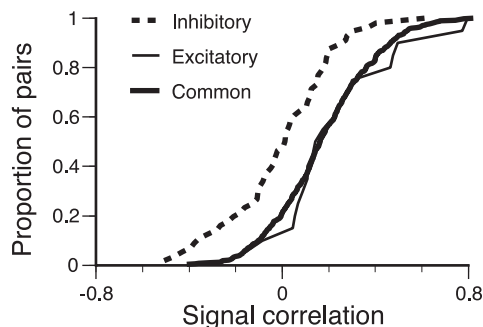


FIG. 10. *A*: cumulative sums of signal correlations for neurons with inhibitory linkages (dotted line), excitatory linkages (thin line), and common inputs (thick line).

neurons have broader spikes (Foehring et al. 1991; Kawaguchi 1995; Thomson et al. 1996). Indeed, some of the identified inhibitory neurons had a broader spike width ( $>400 \mu\text{s}$ ; see Fig. 5). A method used to classify hippocampal neuronal types measures the occurrence of burst spikes (Csicsvari et al. 1999). The occurrence of bursting discharges in the neocortex, however, is not associated with a single neuron type (McCormick et al. 1985). These considerations motivated us to employ cross-correlation analysis to identify inhibitory neurons: identification based solely on spike width would miss a large population of nonfast spiking inhibitory neurons.

We followed protocols outlined in previous reports to interpret CCGs (Bryant et al. 1972; Hata et al. 1990; Menz and Freeman 2003; Moore et al. 1970; Perkel et al. 1967; Toyama et al. 1981; Ts'o et al. 1986). Raw CCGs containing a displaced trough were interpreted as neurons connected through inhibitory linkages; in the pair, the source neuron of this linkage is presumed to be inhibitory. The troughs in raw CCGs

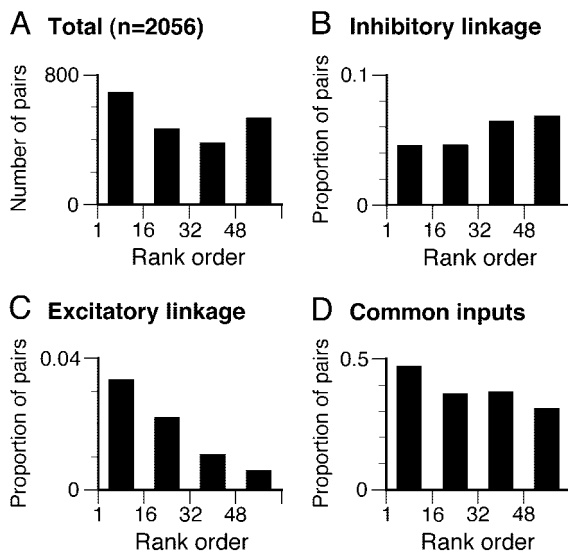


FIG. 11. Frequency distributions of 2,056 stimulus rank orders from all 1,028 pairs (A), 56 inhibitory-linkage pairs (B,  $n = 112$ ), 20 excitatory-linkage pairs (C,  $n = 40$ ), and 397 common-input pairs (D,  $n = 794$ ). We determined the ranking of the most preferred stimulus of a paired neuron in the partner neuron's stimulus preference. The graphs in B–D display the proportions of total pairs falling in each of the 4 rank-order groups so as to eliminate a sampling bias. Bin width was 16. *Far left*: rank orders of 1–15; *middle left*: 16–31; *middle right*: 32–47; *far right*: rank orders of  $\geq 48$ .

of our inhibitory-linkage pairs had width of  $15.0 \pm 11.4$  (SD) ms, similar to values recorded for monosynaptic inhibitory postsynaptic potentials (IPSPs) in cortical neurons (Komatsu et al. 1988; Matsumura et al. 1996). If cross-correlation analysis was to detect polysynaptic connections involving inhibitory neurons, some of our presumed inhibitory neurons may be excitatory neurons. One possibility is that such an excitatory neuron in the recorded pair drives an unobserved inhibitory neuron, which in turn inhibits the other neuron of the pair. Another possibility is that a common excitatory input drives one neuron of the pair directly and inhibits the other neuron via an intervening but unobserved inhibitory neuron. These circuits or variations thereof could in principle cause a trough in the CCG. Although these possibilities cannot be excluded, it is highly unlikely because a polysynaptic CCG is the convolution of successive monosynaptic CCGs (Fetz et al. 1991), and a trough caused by polysynaptic inhibition is significantly diminished. Even monosynaptic inhibitory connections are difficult to detect (Aertsen and Gerstein 1985); previous studies have often failed to detect them (e.g., Gawne and Richmond 1993; Gochin et al. 1991; Rao et al. 1999; but see Constantinidis et al. 2001, 2002; Hata et al. 1988, 1990; Toyama et al. 1981). Further, if cross-correlation analysis detects polysynaptic connections, we would expect to have cases where a single neuron provides excitatory effects on a target neuron and inhibitory effects, via unobserved inhibitory neurons, on another neuron. However, we never observed this. A problem associated with cross-correlation analysis is its inability to detect weak functional interactions (Aertsen and Gerstein 1985; Melssen and Epping 1987). Thus our interpretation of the present results may be restricted to the pairs with strong functional interactions. Although such weak interactions may not be functionally relevant, these limitations must be taken into consideration.

We detected 20 excitatory linkages. Although excitatory

connections prevail in the cortex, such a low incidence of purely direct excitatory linkages is usually the case for cross-correlation analysis (Constantinidis et al. 2001; Hata et al. 1990; Toyama et al. 1981; Ts'o et al. 1986). Cortical neurons constitute a highly interconnected network; each neuron receives inputs from many others, while it provides inputs to many others. In this situation, we can expect that most of the neurons connected with an excitatory linkage also shares synaptic inputs, and a displaced peak of a CCG, which derived from excitatory linkage between them, will be buried in a center common-input peak. In this situation, a broad displaced peak straddling the 0-ms bin or an asymmetric peak can be found in CCG. Such a peak can be interpreted as an indication of a serial linkage. However, it can also be explained by common inputs without direct excitatory linkage. Thus if there is a broad peak straddling the 0-ms bin in a CCG, we cannot be sure about the presence of direct excitatory linkage between the two neurons.

#### Operation mode of inhibition

Local application of bicuculline to TE neurons alters their stimulus selectivity, enhancing their responses to some stimuli but not to others (Wang et al. 2000, 2003). Bicuculline administration often unmasks responses to originally ineffective stimuli, while preserving responses to some of the originally effective stimuli. These results suggest that GABAergic inhibition functions in a stimulus-specific manner. Stimulus-specific inhibition could originate from stimulus-insensitive inhibitory neurons that exert shunting inhibition on target dendrites receiving stimulus-selective excitatory inputs. The present study, however, demonstrated that inhibitory neurons are stimulus selective. Non-stimulus-driven inhibition may also be at work as the spontaneous firing of inhibitory neurons is high (the present study) and the administration of bicuculline mildly increases the spontaneous firing rates (Wang et al. 2000).

Inhibition in a neuron frequently derives from other neurons that, although they may share some of the preferred stimuli (as in Fig. 11B, *far left*), show a low overall signal correlation. Additional groups of neuron pairs (Fig. 11B, *far right*) preferred different stimuli. Thus a neuron receives inhibitory inputs both from neurons sharing some of the preferred stimulus, but with low overall selectivity similarity, and from neurons that do not share preferred stimulus. This is consistent with the results of previous experiments; disinhibition of responses by administration of bicuculline occurs for particular groups of stimuli that are related to the originally effective stimuli and for the stimuli that do not originally excite the neurons themselves but instead activate adjacent neurons (Wang et al. 2000). The present results indicate that some of the source neurons for this inhibition reside in close vicinity of the target neurons, presumably within the same functional column (see following text).

#### Columnar organization in area TE

Stimulus preferences are correlated to a greater extent between adjacent TE neurons than between distant ones (Gochin et al. 1991; Wang et al. 2000). TE neurons responding to similar object images are clustered in columns (Fujita et al. 1992; Tsunoda et al. 2001; Wang et al. 1996). Afferents to a

local region in area TE form columnar clusters (Fujita and Fujita 1996; Miyata et al. 2000; Saleem et al. 1993); adjacent neurons in the local region are likely to share a high proportion of inputs. The present study demonstrates that approximately half of adjacent neuron pairs share common inputs. These pairs have greater stimulus preference similarity than those without common inputs or excitatory linkages.

TE neurons within a column do not necessarily have identical, although similar or correlated, stimulus selectivity with their neighbors. There is heterogeneity in stimulus preference within a column or even between adjacent neurons (Fujita et al. 1992; Gawne and Richmond 1993; Wang et al. 2000). As half of the examined pairs did not share inputs, varied degrees of afferent-input sharing may produce the heterogeneity. Inhibitory interactions between adjacent neurons also contribute to the generation of the heterogeneity.

In area TE, inhibitory neurons can suppress the responses of adjacent target neurons to irrelevant inputs. This kind of local inhibitory interaction may not be specific to area TE. Models for orientation selectivity of primary visual cortex neurons often assume that all neurons in a columnar region respond to the same orientation and that cross-orientation inhibition originates from neurons in different columns with different orientation preferences (Somers et al. 1995; Wörgötter and Koch 1991). Although most adjacent neurons in the primary visual cortex share a preferred orientation, there exist neurons with a wide variety of preferred orientations within a local region (Maldonado and Gray 1996). The question remains if the latter neurons are inhibitory, providing cross-orientation inhibition from within a same columnar region in a similar way as seen in area TE.

#### *Inhibitory neurons in other systems*

Inhibitory neurons in the primary visual cortex are selective for the orientation of stimulus bars or gratings in a similar way as excitatory neurons (Azouz et al. 1997; Gilbert and Wiesel 1979; Kelly and Van Essen 1974; Martin et al. 1983; but see Swadlow 1988). Experimental evidence and theoretical modeling suggest that both cross-orientation and iso-orientation inhibition contribute to shaping orientation selectivity (Blakemore and Tobin 1972; Douglas et al. 1991; Eysel et al. 1990; Ferster 1986; Hata et al. 1988; Kisvárdy et al. 1994; Monier et al. 2003; Sato et al. 1996; Shapley et al. 2003; Sillito 1975; Somers et al. 1995; Wörgötter and Koch 1991).

Stimulus-selective responses of inhibitory neurons have also been demonstrated in the prefrontal cortex. Fast-spiking neurons, which are putative inhibitory neurons, in the primate prefrontal cortex are directionally tuned to a memory target during an oculomotor delayed response task (Rao et al. 1999; Wilson et al. 1994). Fast-spiking neurons in the prefrontal cortex respond to a different direction than regular-spiking neurons located  $\sim 400 \mu\text{m}$  away (Wilson et al. 1994). When comparisons are confined to more closely adjacent neurons recorded at a single site, fast- and regular-spiking neurons have similar directional preferences (Rao et al. 1999). Cross-directional inhibition predominates between functional columns with different directional tuning, while iso-directional inhibition operates within a column.

In summary, evidence from different areas indicates that inhibitory neurons exhibit responses selective for particular

stimulus features or remembered spatial fields in a manner similar to excitatory neurons. They contribute to the formation of response properties of target neurons in a stimulus-specific manner rather than simply controlling the activity levels of the neuronal network.

#### ACKNOWLEDGMENTS

We thank T. Doi, H. Sato, S. Tanabe, and Y. Wang for comments on the manuscript and M. Murayama and K. Miyata for technical assistance.

#### GRANTS

This work was supported by a CREST grant from the Japan Science and Technology Corporation to I. Fujita, grants from the Japanese Ministry of Education, Culture, Sports, Science and Technology to I. Fujita and H. Tamura, and grants from National Institute of Advanced Industrial Science and Technology to H. Tamura and H. Kaneko. Two of the animals used were obtained through the Cooperation Research Program of Primate Research Institute, Kyoto University.

#### REFERENCES

- Aertsen A and Gerstein GL. Evaluation of neuronal connectivity: sensitivity of cross correlation. *Brain Res* 340: 341–354, 1985.
- Azouz R, Gray CM, Nowak LG, and McCormick DA. Physiological properties of inhibitory interneurons in cat striate cortex. *Cereb Cortex* 7: 534–545, 1997.
- Blakemore C and Tobin EA. Lateral inhibition between orientation detectors in the cat's visual cortex. *Exp Brain Res* 15: 439–440, 1972.
- Boussaoud D, Desimone R, and Ungerleider LG. Visual topography of area TEO in the macaque. *J Comp Neurol* 306: 554–575, 1991.
- Bryant HL, Marcos AR, and Segundo JP. Correlations of neuronal spike discharges produced by monosynaptic connections and by common inputs. *J Neurophysiol* 36: 205–225, 1972.
- Constantinidis C, Franowicz MN, and Goldman-Rakic PS. Coding specificity in cortical microcircuits: a multiple-electrode analysis of primate prefrontal cortex. *J Neurosci* 21: 3646–3655, 2001.
- Constantinidis C and Goldman-Rakic PS. Correlated discharges among putative pyramidal neurons and interneurons in the primate prefrontal cortex. *J Neurophysiol* 88: 3487–3497, 2002.
- Constantinidis C, Williams GV, and Goldman-Rakic PS. A role for inhibition in shaping the temporal flow of information in prefrontal cortex. *Nat Neurosci* 5: 175–180, 2002.
- Csicsvari J, Hirase H, Czurkó A, Mamiya A, and Buzsáki G. Oscillatory coupling of hippocampal pyramidal cells and interneurons in the behaving rat. *J Neurosci* 19: 274–287, 1999.
- Desimone R, Albright TD, Gross CG, and Bruce C. Stimulus-selective properties of inferior temporal neurons in the macaque. *J Neurosci* 4: 2051–2062, 1984.
- Douglas RJ, Martin KAC, and Whitteridge D. An intracellular analysis of the visual responses of neurons in cat visual cortex. *J Physiol* 440: 659–696, 1991.
- Eysel UT, Crook JM, and Machemer HF. GABA-induced remote inactivation reveals cross-orientation inhibition in the cat striate cortex. *Exp Brain Res* 80: 626–630, 1990.
- Ferster D. Orientation selectivity of synaptic potentials in neurons of cat primary visual cortex. *J Neurosci* 6: 1284–1301, 1986.
- Fetz E, Toyama K, and Smith W. Synaptic interactions between cortical neurons. In: *Cerebral Cortex*, edited by Peters A and Jones EG, New York: Plenum, 1991, vol. 9, p. 1–49.
- Foehring RC, Lorenzon NM, Herron P, and Wilson CJ. Correlation of physiologically and morphologically identified neuronal types in human association cortex in vitro. *J Neurophysiol* 66: 1825–1837, 1991.
- Fujita I. The inferior temporal cortex: architecture, computation, and representation. *J Neurocytol* 31: 359–371, 2002.
- Fujita I and Fujita T. Intrinsic connections in the macaque inferior temporal cortex. *J Comp Neurol* 368: 467–486, 1996.
- Fujita I, Tanaka K, Ito M, and Cheng K. Columns for visual features of objects in monkey inferotemporal cortex. *Nature* 360: 343–346, 1992.
- Gallant JL, Braun J, and Van Essen DC. Selectivity for polar, hyperbolic and cartesian gratings in macaque visual cortex. *Science* 259: 100–103, 1993.

- Gawne TJ and Richmond BJ.** How independent are the messages carried by adjacent inferior temporal cortical neurons? *J Neurosci* 13: 2758–2771, 1993.
- Gilbert CD and Wiesel TN.** Morphology and intracortical projections of functionally characterized neurons in the cat visual cortex. *Nature* 280: 120–125, 1979.
- Gochin PM, Miller EK, Gross CG, and Gerstein G.** Functional interactions among neurons in inferior temporal cortex of the awake macaque. *Exp Brain Res* 84: 505–516, 1991.
- Gross CG, Rocha-Miranda CE, and Bender DB.** Visual properties of neurons in inferotemporal cortex of the macaque. *J Neurophysiol* 35: 96–111, 1972.
- Hata Y, Tsumoto T, Sato H, Hagihara K, and Tamura H.** Inhibition contributes to orientation selectivity in visual cortex of cat. *Nature* 335: 815–817, 1988.
- Hata Y, Tsumoto T, Sato H, Hagihara K, and Tamura H.** Horizontal interactions between visual cortical neurons studied by cross-correlation analysis in the cat. *J Physiol* 441: 593–614, 1990.
- Hegd  J and Van Essen DC.** Selectivity for complex shapes in primate visual area V2. *J Neurosci* 20: RC1–6, 2000.
- Janssen P, Vogels R, and Orban GA.** Three-dimensional shape coding in inferior temporal cortex. *Neuron* 27: 385–397, 2000.
- Kaneko H, Suzuki SS, Okada J, and Akamatsu M.** Multineuronal spike classification based on multisite electrode recording, whole-waveform analysis, and hierarchical clustering. *IEEE Trans Biomed Eng* 46: 280–290, 1999.
- Kaneko H, Suzuki SS, Tamura H, Takita M, and Akamatsu M.** A micro-electrode positioning system for semiautomatically tracking neuronal spikes. *Proc 20th Conference of IEEE Med Biol* 20: 2236–2238, 1998.
- Kato M, Uka T, and Fujita I.** How selective and reliable are visual responses of inferior temporal cortex neurons? Comparison between anesthetized and awake conditions. *Soc Neurosci Abstr* 25: 918, 1999.
- Kawaguchi Y.** Physiological subgroups of nonpyramidal cells with specific morphological characteristics in layer II/III of rat frontal cortex. *J Neurosci* 15: 2638–2655, 1995.
- Kawasaki K, Tamura H, Miyata K, and Fujita I.** Quantitative comparison of intrahemispheric and interhemispheric responses of area TE neurons in macaques. *Soc Neurosci Abstr* 448.7, 2000.
- Kelly JP and Van Essen DC.** Cell structure and function in the visual cortex of the cat. *J Physiol* 238: 515–547, 1974.
- Kisv rdy ZF, Kim D-S, Eysel UT, and Bonhoeffer T.** Relationship between lateral inhibitory connections and the topography of the orientation map in cat visual cortex. *Eur J Neurosci* 6: 1619–1632, 1994.
- Kobatake E and Tanaka K.** Neuronal selectivities to complex object features in the ventral visual pathway of the macaque cerebral cortex. *J Neurophysiol* 71: 856–867, 1994.
- Komatsu H, Ideura Y, Kaji S, and Yamane S.** Color selectivity of neurons in the inferior temporal cortex of the awake macaque monkey. *J Neurosci* 12: 408–424, 1992.
- Komatsu Y, Nakajima S, Toyama K, and Fetz EE.** Intracortical connectivity revealed by spike-triggered averaging in slice preparations of cat visual cortex. *Brain Res* 442: 359–362, 1988.
- Lance GN and Williams WT.** A general theory of classificatory sorting strategies. I. Hierarchical systems. *Comput J* 9: 373–380, 1967.
- Logothetis NK, Guggenberger H, Peled S, and Pauls J.** Functional imaging of the monkey brain. *Nat Neurosci* 2: 555–562, 1999.
- Maldonado PE and Gray CM.** Heterogeneity in local distributions of orientation-selective neurons in the cat primary visual cortex. *Vis Neurosci* 13: 509–516, 1996.
- Martin KAC, Somogyi P, and Whitteridge D.** Physiological and morphological properties of identified basket cells in the cat's visual cortex. *Exp Brain Res* 50: 193–200, 1983.
- Matsumura M, Chen D-F, Sawaguchi T, Kubota K, and Fetz EE.** Synaptic interactions between primate precentral cortex neurons revealed by spike-triggered averaging of intracellular membrane potentials in vivo. *J Neurosci* 16: 7757–7767, 1996.
- McCormick DA, Connors BW, Lighthall JW, and Prince DA.** Comparative electrophysiology of pyramidal and sparsely spiny stellate neurons of the neocortex. *J Neurophysiol* 54: 782–806, 1985.
- Melssen WJ and Epping WJM.** Detection and estimation of neuronal connectivity based on cross-correlation analysis. *Biol Cybern* 57: 403–414, 1987.
- Menz DM and Freeman RD.** Stereoscopic depth processing in the visual cortex: a coarse-to-fine mechanisms. *Nat Neurosci* 6: 59–65, 2003.
- Miyata K, Kawasaki K, Wang QX, Tamura H, and Fujita I.** Columnar interhemispheric connections between area TEs in macaque. *Soc Neurosci Abstr* 448.6, 2000.
- Monier C, Chavane F, Baudot P, Graham LJ, and Fr gnac Y.** Orientation and direction selectivity of synaptic inputs in visual cortical neurons: a diversity of combinations produces spike tuning. *Neuron* 37: 663–680, 2003.
- Moore GP, Segundo JP, Perkel DH, and Levitan H.** Statistical signs of synaptic interaction in neurons. *Biophys J* 10: 876–900, 1970.
- Mountcastle VB, Talbot WH, Sakata H, and Hyv rinen J.** Cortical neuronal mechanisms in flutter-vibration studied in unanesthetized monkeys. Neuronal periodicity and frequency discrimination. *J Neurophysiol* 32: 452–484, 1969.
- Pack CC, Berezovskii VK, and Born RT.** Dynamic properties of neurons in cortical area MT in alert and anesthetized macaque monkey. *Nature* 414: 905–908, 2001.
- Pasupathy A and Connor CE.** Responses to contour features in macaque area V4. *J Neurophysiol* 82: 2490–2502, 1999.
- Perkel DH, Gerstein GL, and Moore GL.** Neuronal spike trains and stochastic point processes. II. Simultaneous spike trains. *Biophys J* 7: 419–440, 1967.
- Perrett DI, Rolls ET, and Caan W.** Visual neurons responsive to faces in the monkey temporal cortex. *Exp Brain Res* 47: 329–342, 1982.
- Popilskis SJ and Kohn DF.** Anesthesia and analgesia in nonhuman primates. In: *Anesthesia and Analgesia in Laboratory Animals*, edited by Kohn DF, Wixon SK, White WJ, and Benson GJ. New York: Academic, 1999, p. 233–255.
- Rao SG, Williams GV, and Goldman-Rakic PS.** Isodirectional tuning of adjacent interneurons and pyramidal cells during working memory: evidence for microcolumnar organization in PFC. *J Neurophysiol* 81: 1903–1916, 1999.
- Rodman HR, Skelly JP, and Gross CG.** Stimulus selectivity and state dependence of activity in inferior temporal cortex of infant monkeys. *Proc Natl Acad Sci USA* 88: 7572–7575, 1991.
- Saleem KS, Tanaka K, and Rockland KS.** Specific and columnar projection from area TEO to TE in the macaque inferotemporal cortex. *Cereb Cortex* 3: 454–464, 1993.
- S ry G, Vogels R, Kovacs G, and Orban GA.** Responses of monkey inferior temporal neurons to luminance-, motion-, and texture-defined gratings. *J Neurophysiol* 73: 1341–1354, 1995.
- Sato H, Katsuyama N, Tamura H, Hata Y, and Tsumoto T.** Mechanisms underlying orientation selectivity of neurons in the primary visual cortex of the macaque. *J Physiol* 494: 757–771, 1996.
- Shapley R, Hawken M, and Ringach DL.** Dynamics of orientation selectivity in the primary visual cortex and the importance of cortical inhibition. *Neuron* 38: 689–699, 2003.
- Sillito AM.** The contribution of inhibitory mechanisms to the receptive field properties of neurons in the striate cortex of the cat. *J Physiol* 250: 305–329, 1975.
- Simons DJ.** Response properties of vibrissa units in rat SI somatosensory neocortex. *J Neurophysiol* 41: 798–820, 1978.
- Somers DC, Nelson SB, and Sur M.** An emergent model of orientation selectivity in cat visual cortical simple cells. *J Neurosci* 15: 5448–5465, 1995.
- Swadlow HA.** Efferent neurons and suspected interneurons in binocular visual cortex of the awake rabbit: receptive fields and binocular properties. *J Neurophysiol* 59: 1162–1187, 1988.
- Tamura H, Kaneko H, Kawasaki K, and Fujita I.** Visual response properties of presumed inhibitory neurons in the inferior temporal cortex of macaque monkey. *Soc Neurosci Abstr* 160.7, 2002.
- Tamura H and Tanaka K.** Visual response properties of cells in the ventral and dorsal parts of the macaque inferotemporal cortex. *Cereb Cortex* 11: 384–399, 2001.
- Tanaka K, Saito H-A, Fukada Y, and Moriya M.** Coding visual images of objects in the inferotemporal cortex of the macaque monkey. *J Neurophysiol* 66: 170–189, 1991.
- Thomson AM, West DC, Hahn J, and Deuchars J.** Single axon IPSPs elicited in pyramidal cells by three classes of interneurons in slices of rat neocortex. *J Physiol* 496: 81–102, 1996.
- Tigwell DA and Sauter J.** On the use of isoflurane as an anesthetic for visual neurophysiology. *Exp Brain Res* 88: 224–228, 1992.
- Toyama K, Kimura M, and Tanaka K.** Cross-correlation analysis of inter-neuronal connectivity in cat visual cortex. *J Neurophysiol* 46: 191–201, 1981.

- Ts'o DY, Gilbert CD, and Wiesel TN.** Relationships between horizontal interactions and functional architecture in cat striate cortex as revealed by cross-correlation analysis. *J Neurosci* 6: 1160–1170, 1986.
- Tsunoda K, Yamane Y, Nishizaki M, and Tanifuji M.** Complex objects are represented in macaque inferotemporal cortex by the combination of feature columns. *Nat Neurosci* 4: 832–838, 2001.
- Uka T, Tanaka H, Yoshiyama K, Kato M, and Fujita I.** Disparity selectivity of neurons in monkey inferior temporal cortex. *J Neurophysiol* 84: 120–132, 2000.
- Wang G, Tanaka K, and Tanifuji M.** Optical imaging of functional organization in the monkey inferotemporal cortex. *Science* 272: 1665–1668, 1996.
- Wang Y, Fujita I, and Murayama Y.** Neuronal mechanisms of selectivity for object features revealed by blocking inhibition in inferotemporal cortex. *Nat Neurosci* 3: 807–813, 2000.
- Wang Y, Fujita I, and Murayama Y.** Coding of visual patterns and textures in monkey inferior temporal cortex. *NeuroRep* 14: 453–458, 2003.
- Wang Y, Fujita I, Tamura H, and Murayama Y.** Contributions of GABAergic inhibition to receptive field structures of monkey inferior temporal neurons. *Cereb Cortex* 12: 62–74, 2002.
- Wilson FAW, O'Scalaidhe SP, and Goldman-Rakic PS.** Functional synergism between putative  $\gamma$ -aminobutyrate-containing neurons and pyramidal neurons in prefrontal cortex. *Proc Natl Acad Sci USA* 91: 4009–4013, 1994.
- Wörgötter F and Koch C.** A detailed model of the primary visual pathway in the cat: comparison of afferent excitatory and intracortical inhibitory connection schemes for orientation selectivity. *J Neurosci* 11: 1959–1979, 1991.